'Added Mass' Vortex Sheet Development in an Accelerating Incident Flow

Pascal Gehlert * and Holger Babinsky †
University of Cambridge, Cambridge, United Kingdom, CB2 1PZ

I. Introduction

The time-variation of unsteady flow around flapping wings [1] or during wing gust encounters [2] significantly complicates the aerodynamics involved [3] and can make it especially difficult to correctly identify the force response. One possible approach to compute this unsteady force is the *impulse* method proposed by Wu [4]. He extended principles first developed by Lamb [5], and showed that the relative motion and change in strength of vorticity within the flow field can be related to a force. Moreover, in a bid to more easily model these complex unsteady phenomena, the flow field is often described using potential flow theory. Here, a true viscous flow field is modelled by superposing individual flow elements, where free vorticity is represented by point vortices and the boundary layer vorticity is modelled as an infinitely thin vortex sheet located on the object's surface [6]. The strength of this vortex sheet matches the vorticity distribution of the original viscous boundary layer and simultaneously enforces the no-through flow condition along its length, thereby itself becoming a streamline. Alternatively, the vortex sheet can be associated with the slip velocity along an object's surface [7].

Just as the flow field can be considered to be a superposition of individual flow elements, the boundary layer vortex sheet can equally be modelled as a superposition of independent contributions, as extensively discussed by Eldredge [8], where each enforces the no-throughflow boundary condition along the object's surface due to a particular flow element. Broadly speaking, the boundary layer vortex sheet γ^b can be grouped into two components. The first is created in response to any free vorticity, effectively acting as a *mirror image*. The second vortex sheet contribution arises from the motion kinematics, and in the absence of rotation, is created in a response to body acceleration. As a body surges, this vortex sheet grows and its rate of change can be related to an *added* (or *apparent) mass* force that describes the additional force required to accelerate an object surrounded by a fluid compared to when it is accelerated in a vacuum [9–11]. To reflect this link between the vortex sheet and the added mass force when the body accelerates, we choose to call this an *added mass* vortex sheet γ^{am} throughout this work, where its distribution can be found from

*Postdoctoral Researcher, Department of Engineering, University of Cambridge, AIAA Student Member, pg469@cam.ac.uk
†Professor of Aerodynamics, Department of Engineering, University of Cambridge, AIAA Fellow, hb@eng.cam.ac.uk

potential flow theory and recovered under experimental conditions [12, 13]. Added mass force is a useful concept since it is easy to calculate and when acceleration rates are large, it captures the main unsteady force contribution [14, 15]. Moreover, viewing the boundary layer vorticity as a superposition of individual vortex sheets, where the rate of change of each component links to a force, has been beneficial in understanding unsteady flows and provides an incentive to correctly identify these [7, 16, 17].

When a stationary body is immersed in an accelerating freestream, the developing boundary layer vortex sheet can be computed from potential flow theory (until separation occurs). In fact, it is precisely identical to the added mass vortex sheet predicted when the object accelerates in stationary flow. At first glance, this is to be expected, since the relative flow velocity around the object is the same. Consequently, an equivalent force can be calculated (together with an additional buoyancy force arising from the pressure gradient within the flow). However, despite being equivalent to the added mass force in magnitude, it is not obvious that this force should be described as such, because the object has not accelerated. An example of this is ambiguity is encountered in Küssner's model, predicting the force during a flat plate sharp-edged gust encounter [18, 19], where von Kármán and Sears [20] isolate an *apparent* or *added mass* force during gust entry (and exit), despite the plate not accelerating. Furthermore, an accelerating flow is generally not of infinite extent and there must therefore be some vorticity along its outer boundary. Like any other free vorticity, this should equally contribute to the boundary layer vortex sheet and thus the resulting force. Therefore, two questions naturally arise:

1) How should this external vorticity be treated?
2) What is the true origin of the so called *added mass* force when the surrounding fluid, rather than the body, accelerates?

The correct definition of an added mass force may appear a trivial problem of semantics, however, an incorrect attribution of boundary layer vortex sheet components to flow features and kinematics may lead to invalid conclusions when trying to decompose the force or isolate boundary layer vortex sheet contributions. In unsteady scenarios it may be tempting to explicitly include an *added / apparent* mass force whenever the flow accelerates. However, if at the same time the flow field includes externally generated vorticity, residing for example in wind tunnel boundary- or gust shear layers, and the time variation of the associated vortex sheet is evaluate to yield a force then the same force is considered twice, leading to 'double counting'. It is thus crucial that the correct origin of boundary layer vorticity is identified. The aim of this note is therefore to explore this problem experimentally on a flat plate perpendicular to an accelerating flow to answer the above questions.

The experiments are conducted in the Cambridge University towing tank, which is 9 m long, 1 m wide and filled to a height of 0.8 m. A carbon fibre plate is equipped with two forward directed 0.135 m long side skirts that enclose the region around a stationary flat plate. The side skirts are 3D printed using ABS plastic with a thickness t of 0.005 m, a

total span of 0.235 m and a width of 0.14 m. A see-through piece of perspex is placed at the midspan location of the side skirts to allow a laser sheet to illuminate the flow. The stationary aluminium flat plate has a span of 0.48 m, a thickness w of 0.005 m and a chord length c of 0.045 m.

The scoop, which is mounted to a carriage that runs along the length of the tank, accelerates at a constant rate over a distance of one plate chord (0.045 m) to a final velocity of of 0.11 ms^{-1}, or an equivalent Reynolds number of 4000, whilst the plate is held in place by an external support.

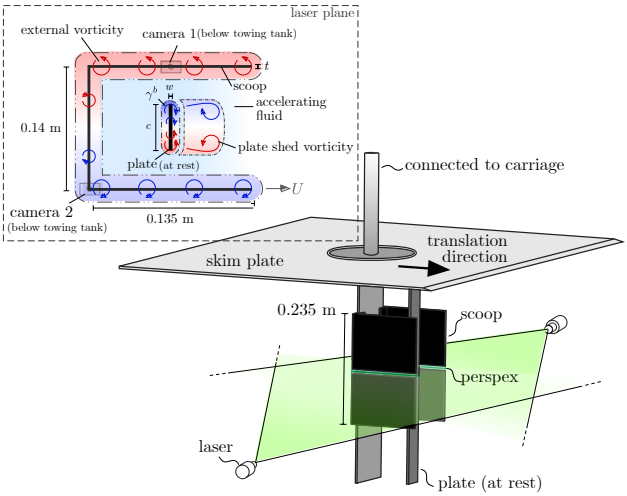

Fig. 1 Scoop set-up.

Planar PIV is used interrogate the flow field using a dual laser sheet approach shown towards the bottom of figure 1. Titanium dioxide particles are illumined using an Nd:YLF 572 nm laser and two high speed Phantom M310 cameras are used for data acquisition. The sampling frequency of the images is 200 Hz, which are post-processed using the commercial LaVision Flow Master 2D system. A multi-pass adaptive interrogation window is used with a size of 16×16 pixels during its final pass and an overlap ratio of 50 %, leading to a vector spacing of 2.6 mm. The velocity vectors of each camera are stitched together and linearly averaged over any overlapping regions. To remove any shadow regions in the acquired data, camera 1 is aligned with one of the side skirts as well as the stationary flat plate, as illustrated in figure 1. This provides the optical access to the region extending to the back wall of the scoop and the opposing skirt. To capture the remaining flow field, camera 2 is placed at the opposing corner, such that it is in line with the back of the scoop as well as the second side skirt, when the scoop is in its initial starting position. Together, the cameras are able to capture the complete flow field, and the final velocity vectors are averaged from 8 independent runs.

II. Surface Vortex Sheet

A. Freestream Velocity

The finite nature of the scoop leads to an incident velocity on the stationary plate which not only varies in time as the scoop accelerates but one that is also related to the relative position between the scoop and plate, due to 'spillage' along the front end of the scoop and spanwise flow. The reasonably large blockage ratio of 32 % between plate and scoop prevents a sampling of the inflow velocity by simply repeating the same motion kinematics of the scoop in the absence of the plate. Instead, we propose to determine the *effective* velocity of the incident flow from the instantaneous vorticity field created by the motion of the scoop. Since the velocity at any position in space can be understood as a superposition of that induced by each individual vortical element according to the Biot-Savart law [6] we can estimate the effective flow velocity by computing the velocity induced at the midchord from the vorticity distribution associated with the surging scoop for each time step. An example of the relevant vorticity field is seen in figure 2 when the scoop has moved 0.2 and 1.4 chord lengths, s/c, showing positive and negative vorticity forming along the scoop edges, whilst at the same time vorticity sheds from either side of the plate and begins to roll up into two distinct vortices.

Comparing the result to the *ideal* and actual *scoop* velocity in figure 2 shows that the effective velocity experienced by the plate lags behind the velocity of the scoop itself. This appears to be predominately due to 'spillage' since PIV measurements 1 cm (or 0.22c) in front of the plate found negligible spanwise flow. Therefore whilst the short span and length of the scoop introduce some untidiness into the data, the velocity correction outlined above should render any adverse affects due to a velocity gradient within the scoop minute.

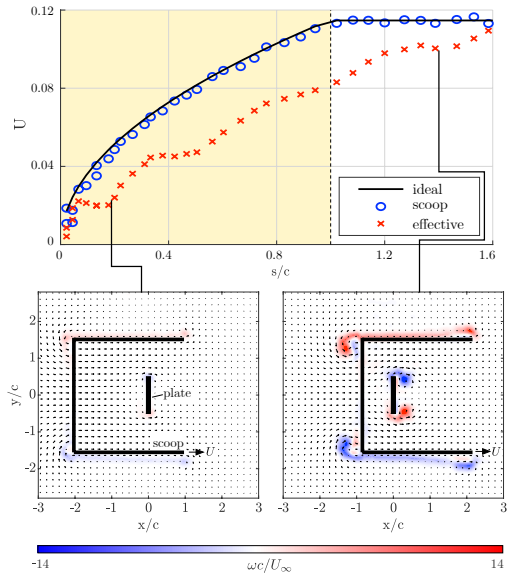

Fig. 2 Incident flow velocity as well as vorticity contour snapshots at $s/c = 0.2$ and 1.4.

B. 'Added Mass'-Like Vortex Sheet

To begin the analysis of the origin of the surface vortex sheet, we initially assume that the stationary plate is immersed in an unbounded freestream, as modelled when using conventional potential flow. The flow field is therefore assumed to only consist of boundary layer vorticity as well as any vorticity shed from the plate. The total vortex sheet γ^b can therefore be expressed as $\gamma^b = \gamma + \gamma^{shed}$, where γ is a place holder for the supposed 'added-mass'-like vortex sheet and γ^{shed} is created in response to plate-shed vorticity . To isolate γ, we identify γ^{shed} and remove this from the total boundary vortex sheet γ^b [12],

$$\gamma = \gamma^b - \gamma^{shed}. \tag{1}$$

To measure γ^b, we discretize the plate and the surrounding flow field into 70 rectangles with a height δh_k of $0.2c$, as shown in the insert in figure 3. The vortex sheet strength $\delta\gamma_k^b$ at each element is found by integrating the velocity aligned with the contour of each rectangular segment to get an elemental circulation $\delta\Gamma_k$. This is subsequently divided by the element width δs_k to arrive at the vortex sheet strength, $\delta\gamma_k^b = \delta\Gamma_k/\delta s_k$ [12]. γ^{shed} is obtained by identifying the surface slip velocity along the plate surface induced by each element of vorticity shed by the plate [16]. The theoretical distribution of the *added mass* vortex sheet is given by,

$$\gamma_{theory}^{am} = -2U_n \frac{x}{\sqrt{(c/2)^2 - x^2}}, \tag{2}$$

where U_n is the plate normal velocity and x is a position along its chord [21].

A comparison between the theoretical and experimental distributions is shown towards the left of figure 3 *. Since the added mass vortex sheet scales with velocity (equation 2), noise in the measurements can be reduced by taking the average of the vortex sheet measured at each instance in time divided by instantaneous velocity. We show the results when the experimental vortex sheet is scaled using both the *scoop* as well as the *effective* velocity, where the latter is recovered from external vorticity using the method discussed in section II.A.

*It is noted that due to the rather coarse resolution of the PIV data, resulting from the large field of view required to measure the complete flow field, data presented in the left of figure 3 are from $s/c > 0.5$ onwards, when the boundary layer and shed vorticity can be distinguished.

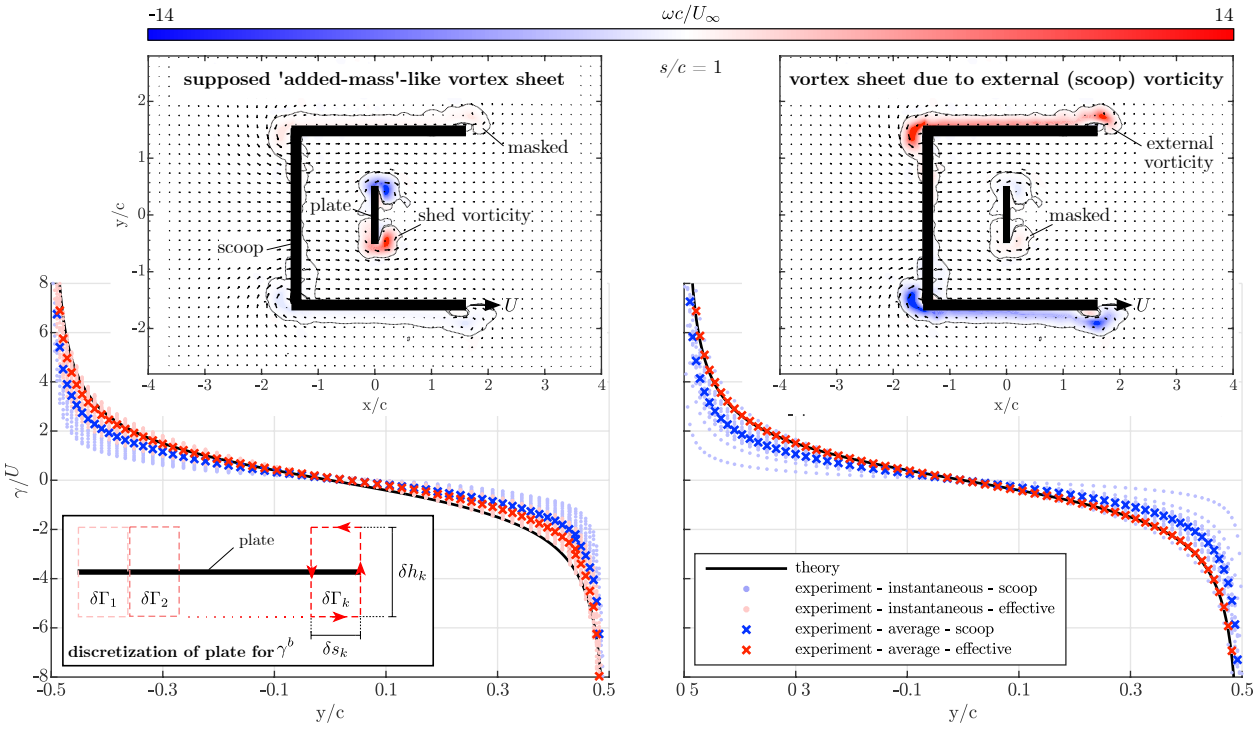

Fig. 3 Plate vortex sheets

The general shape of both experimental vortex sheets closely follows the theoretical distribution albeit at a slightly reduced magnitude. The larger discrepancy to theory observed when scaling the vortex sheet by scoop velocity can be attributed to the mismatch between the velocity of the scoop and that felt by the plate, as previously observed in figure 2. Despite this small difference, it is clear from the left of figure 3 that an 'added-mass-like' vortex sheet does in fact form on the stationary flat plate, and its rate of change could in turn be linked to a 'supposed' added mass force. At this point however, we must not forget that up until now we assumed an unbounded freestream and have neglected the effect of any external vorticity created along the scoop. Since there is no conceptual difference between plate-shed or scoop vorticity, there is no viable reason as to why this should be treated differently. We therefore proceed to evaluate the effect that external vorticity has on the boundary layer vortex sheet next.

C. Vortex Sheet to due External (Scoop) Vorticity

To isolate the vortex sheet γ^{ext} created by external vorticity, we use the same methodology previously used to recover γ^{shed}. Rather than assessing plate-shed vorticity, we now evaluate the effect of external vorticity highlighted towards the top right of figure 3 at each instance in time. Again we use both the actual scoop velocity and the *effective* counterpart to scale the resulting vortex sheet distribution at each instance in time. As shown on the bottom right figure 3, the time-averaged distributions are remarkably similar to the theoretical added mass vortex sheet. This implies that the vortex sheet previously observed on the left of figure 3, when assuming an unbounded freestream, is actually a response

to vorticity that forms at the edge of the accelerating freesteam rather than due to any non-existent body acceleration. This result may in hindsight appear trivially obvious, as in the absence of body motion, there is no other source that could have created the vortex sheet. In turn, the boundary layer vortex sheet for the plate immersed in the accelerating freestream can be written as,

$$\gamma^b = \underbrace{\cancel{\gamma^{am}}}_{=0} + \gamma^{shed} + \gamma^{ext}, \tag{3}$$

where the contribution γ^{am}, formally referred to as the *added mass* component, is zero. Instead γ^{ext}, created by external vorticity arising from the accelerating freestream, is the responsible entity for the characteristic 'added-mass'-like distribution. This interpretation is in line with theoretical results from Corkery [22], who mathematically represented an accelerating flow through an external vortex pair that induces a uniform freestream onto a stationary cylinder. The vortex sheet contribution found by directly assessing the vortex pair is identical to an 'added-mass'-like distribution and the experimental results discussed here are thus consistent with his theoretical approach. The results further match Corkery and Babinsky [23] who concluded that the *added mass* vortex sheet, and its associated force, arising during a gust encounter are in fact caused by vorticity residing within the gust shear layers rather than any non-existent body acceleration, with the findings since then extended to arbitrary bodies of volume [24].

On a final note, and shifting the focus to the scoop itself, the *added mass* force associated with its acceleration could be found by isolating and evaluating the time rate of change of its vortex sheet related to kinematic motion.

III. Conclusion

An accelerating flow past a stationary plate is designed such that the complete vorticity field can be measured using planar particle image velocimetry. By assessing the vorticity field it is found that the external vorticity created at the interface of the moving fluid and the quiescent surrounding is responsible for a boundary layer vortex sheet component that looks akin to the *added mass* vortex sheet observed when the plate accelerates. Care must therefore be taken in experiments or simulations to ensure that each boundary layer vortex sheet contribution and its related force is only considered once, as otherwise a 'double counting' of forces can obscure the correct results.

Acknowledgments

The authors would like to acknowledge the Engineering and Physical Science Research Council (EPSRC) for providing financial support.

References

[1] Liu, L.-g., Du, G., and Sun, M., "Aerodynamic-force production mechanisms in hovering mosquitoes," Vol. 2, 2020. doi:https://10.1017/jfm.2020.386.

[2] Andreu-Angulo, I., Babinsky, H., Biler, H., Sedky, G., and Jones, A. R., "Effect of Transverse Gust Velocity Profiles," *AIAA Journal*, Vol. 58, No. 12, 2020, pp. 5123–5133. doi:https://10.2514/1.J059665.

[3] Eldredge, J. D., and Jones, A. R., "Leading-Edge Vortices: Mechanics and Modeling," *Annual Review of Fluid Mechanics*, Vol. 51, No. 1, 2019, pp. 75–104. doi:https://10.1146/annurev-fluid-010518-040334.

[4] Wu, J. C., "Theory for Aerodynamic Force and Moment in Viscous Flows," *AIAA Journal*, Vol. 19, No. 4, 1981, pp. 432–441. doi:https://10.2514/3.50966.

[5] Lamb, H., *Hydrodynamics*, 1932.

[6] Saffman, P. G., *Vortex Dynamics*, Cambridge University Press, 1992.

[7] Eldredge, J. D., "A Reconciliation of Viscous and Inviscid Approaches to Computing Locomotion of Deforming Bodies," *Experimental Mechanics*, Vol. 50, No. 9, 2010, pp. 1349–1353. doi:https://10.1007/s11340-009-9275-0.

[8] Eldredge, J. D., *Mathematical Modeling of Unsteady Invscid Flows*, Springer, 2019.

[9] Darwin, C., "Note on Hydrodynamics," *Mathematical Proceedings of the Cambridge Philosophical Society*, Vol. 49, No. 2, 1953, pp. 342–354. doi:https://10.1017/S0305004100028449.

[10] Blevins, R. D., *Flow-Induced Vibration*, van Nostrand Reinhold, New York, 1977.

[11] Brennen, C. E., "A Review of Added Mass and Fluid Inertial Forces," *Ocean Engineering*, , No. January, 1982, p. 50. doi:http://resolver.caltech.edu/CaltechAUTHORS:BREncel82.

[12] Corkery, S. J., Babinsky, H., and Graham, W. R., "Quantification of Added-Mass Effects Using Particle Image Velocimetry Data for a Translating and Rotating Flat Plate," *Journal of Fluid Mechanics*, Vol. 870, 2019, pp. 492–518. doi:https://10.1017/jfm.2019.231.

[13] Gehlert, P., and Babinsky, H., "Linking the Unsteady Force Generation to Vorticity for a Translating and Rotating Cylinder," *AIAA Scitech 2019 Forum*, 2019. doi:https://10.2514/6.2019-0347.

[14] Gehlert, P., Andreu-Angulo, I., and Babinsky, H., "Unsteady Vorticity Force Decomposition-Evaluating Gust Distortion," *AIAA Scitech 2021 Forum*, 2021, pp. 1–23. doi:https://10.2514/6.2021-1084.

[15] Limacher, E. J., "Added-mass force on elliptic airfoils," *Journal of Fluid Mechanics*, Vol. 926, 2021, pp. 1–12. doi:https://10.1017/jfm.2021.741.

[16] Graham, W. R., Pitt Ford, C. W., and Babinsky, H., "An Impulse-Based Approach to Estimating Forces in Unsteady Flow," *Journal of Fluid Mechanics*, Vol. 815, 2017, pp. 60–76. doi:https://10.1017/jfm.2017.45.

[17] Gehlert, P., and Babinsky, H., "Boundary Layer Vortex Sheet Evolution Around an Accelerating and Rotating Cylinder," *Journal of Fluid Mechanics*, Vol. 915, 2021, pp. 1–20. doi:https://10.1017/jfm.2021.121.

[18] Küssner, H. G., "Stresses produced in Airplane Wings by Gusts," *National Advisory Committee for Aeronautics*, Vol. 654, 1932.

[19] Küssner, H. G., "Untersuchung der Bewegung einer Platte beim Eintritt in eine Strahlgrenze," *Zentrale für techn.-wiss. Berichtswesen*, Vol. 13, 1936, pp. 425–429.

[20] von Karman, T., and Sears, W. R., "Airfoil Theory for Non-Uniform Motion," *Journal of the Aeronautical Sciences*, Vol. 5, 1938.

[21] Milne-Thomson, L. M., *Theoretical Hydrodynamics*, Courier Corporation, 1996.

[22] Corkery, S. J., "Unsteady Aerodynamics of Wing Gust Encounters," Phd thesis, University of Cambridge, 2019.

[23] Corkery, S. J., and Babinsky, H., "An Investigation into the Added Mass Force for a Transverse Wing-Gust Encounter," *AIAA Scitech 2019 Forum*, 2019. doi:https://10.2514/6.2019-1145.

[24] Gehlert, P., and Babinsky, H., "Noncirculatory Force on a Finite Thickness Body Encountering a Gust," *AIAA Journal*, Vol. 59, No. 2, 2021, pp. 719–730. doi:https://10.2514/1.J059686.